Dissection of the Extracellular Human Interferon γ Receptor α-Chain into two Immunoglobulin-like Domains. Production in an *Escherichia coli* Thioredoxin Gene Fusion Expression System and Recognition by Neutralizing Antibodies†

Geoffrey Williams,‡ Nicole Ruegg,‡ Ashley Birch,‡ Christoph Weber,‡ Klaus Hofstädter,‡ John A. Robinson,*,‡ Michel Aguet,§,|| Gianni Garotta,⊥ Daniel Schlatter,⊥ and Walter Huber⊥

Institute of Organic Chemistry, University of Zürich-Irchel, 8057 Zürich, and Institute of Molecular Biology-I, University of Zürich, Hönggerberg, 8093 Zürich, Switzerland, and Pharma Division, Preclinical Research, F. Hoffmann-La Roche, 4002 Basel, Switzerland

Received August 31, 1994; Revised Manuscript Received November 21, 1994®

ABSTRACT: The extracellular interferon γ receptor α-chain (IFNγR) is believed to comprise two discrete ≈110 amino acid immunoglobulin-like domains, perhaps similar to those seen in the crystal structure of the extracellular human growth hormone receptor [De Vos, A. M., Ultsch, M., & Kossiakoff, A. (1992) *Science 255*, 306−312], a distant relative in the cytokine receptor superfamily. In accord with this idea, we show that these IFNγR immunoglobulin-like domains can be produced separately in a soluble form with a native-like fold. The N-terminal domain (residues 1−108), with a Cys^{105} to Ser^{105} mutation, was produced at a high level, in a soluble form, as a thioredoxin−interferon γ receptor fragment fusion protein in the cytoplasm of *Escherichia coli*. Upon extraction, the receptor Cys^{60}−Cys^{68} disulfide bond formed spontaneously, to generate a native-like structure directly without the need for refolding. Cleavage of the fusion protein by enterokinase released the receptor fragment (≈12 kDa), which was recognized by several neutralizing antibodies with affinities, measured using surface plasmon resonance technology, that were essentially indistinguishable from those seen with the full length extracellular IFNγR produced in eukaryotic cells. Circular dichroism and 1D ^{1}H nuclear magnetic resonance spectra indicated that the receptor fragment adopts a folded state, with mainly β-sheet and reverse turn secondary structure. The second membrane-proximal Ig-like domain of the IFNγR (residues 90−229) was produced, albeit less efficiently, and characterized in a similar way. The production of these two independently folded proteins provides experimental support for the two domain organization of the IFNγR and opens new avenues for structural studies on these Ig-like molecules by NMR and crystallographic methods.

The diverse functions of interferon γ (IFNγ)[1] in host defense, inflammation, and autoimmunity arise through its association with species-specific glycoprotein receptors present in low numbers on a wide variety of cells (Farrar & Schreiber, 1993; Langer & Pestka, 1988). The IFNγ receptor α-chain (IFNγR), which is responsible for binding IFNγ at the cell surface, has only a very limited sequence similarity to other members of the hematopoietic cytokine receptor superfamily. Nevertheless, the ligand binding portions of these cytokine receptors are believed to adopt discrete ≈110-amino acid domains, each with an antiparallel β-sandwich topology (Figure 1A) closely related to that of the immunoglobulin (Ig) constant domain (Bazan, 1990a,b; Taga & Kishimoto, 1992). The two-domain organization of the extracellular human growth hormone receptor (GRHR) (De Vos et al., 1992) and tissue factor (Harlos et al., 1994; Muller et al., 1994) were confirmed recently by crystallographic analyses. However, the folding topology of each was identical to that of domain D2 of CD4 and domain D2 of chaperone protein PapD, rather than the Ig-constant domain (Figure 1B). We report here the molecular dissection of the extracellular IFNγR into two soluble recombinant proteins, corresponding in length to the two putative Ig-like domains, each of which has been produced in *Escherichia coli* with native-like properties using a thioredoxin gene fusion expression system.

The human IFNγR is a 90-kDa transmembrane glycoprotein which binds human IFNγ with high affinity ($K_D \approx 10^{-10}$ M) and comprises an extracellular portion of ≈229 amino acid residues, a single transmembrane region of 22 residues, and an intracellular region of 221 residues. It does not require glycosylation in order to bind IFNγ, and the recombinant extracellular portion alone, as well as the intact membrane bound receptor, binds IFNγ tightly in a 2:1 receptor/ligand stoichiometry (Fountoulakis et al., 1992; Greenlund et al., 1993). However, IFNγ-induced signal transduction requires a species-specific interaction of the α-chain with a separate transmembrane receptor β-subunit (Bohni et al., 1994; Gibbs et al., 1991; Hemmi et al., 1992, 1994; Hibino et al., 1992; Soh et al., 1994), and additional receptor subunits may be required to mediate the antiviral actions of IFNγ (Soh et al., 1994). cDNAs for the human

† This work was supported by Grant 5002-34637 from the Swiss National Science Foundation.

* Address correspondence to this author.
‡ Institute of Organic Chemistry.
§ Institute of Molecular Biology-I.
|| Current address : Genentech Inc., 460 San Bruno Blvd., S. San Francisco, CA 94080 USA.
⊥ F. Hoffmann-La Roche.

® Abstract published in *Advance ACS Abstracts,* January 15, 1995.

[1] Abbreviations: IFNγ, interferon γ; IFNγR, interferon γ receptor α-chain; GRH, growth hormone; GRHR, growth hormone receptor; Ig, immunoglobulin; Trx, thioredoxin; PCR, polymerase chain reaction; SPR, surface plasmon resonance; PDI, protein disulfide isomerase.

0006-2960/95/0434-1787$09.00/0

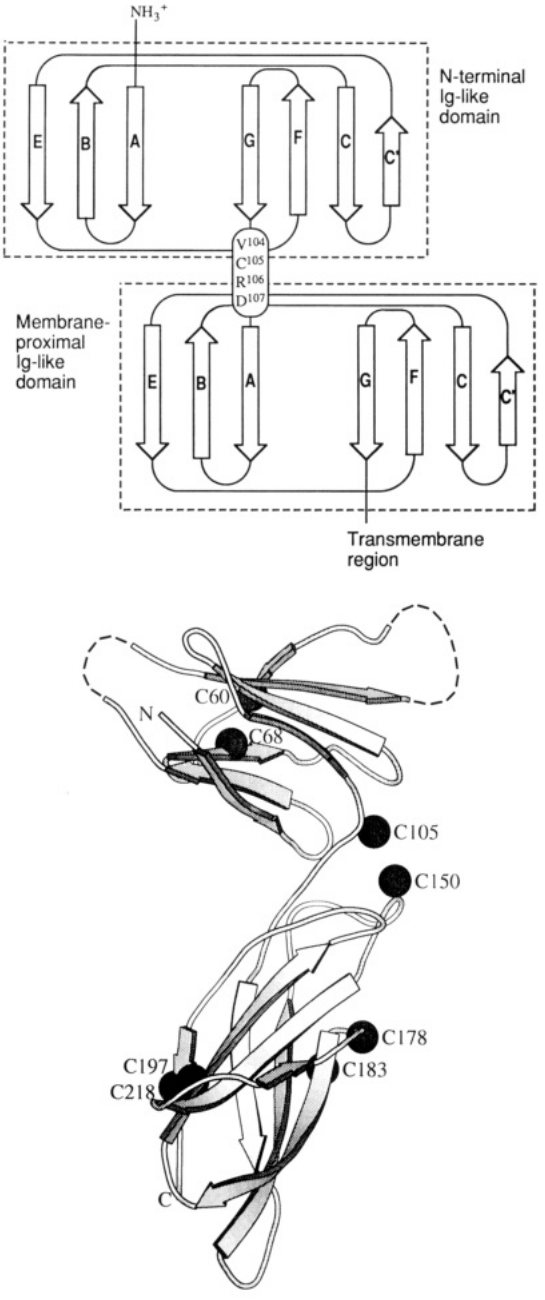

FIGURE 1: (A, top) One possible topology for the Ig-like domains in the extracellular IFNγR. Strands A, B, and E would belong to one sheet and C, C′, F, and G to the other sheet; based on a presumed structural similarity with the GRHR, together with the sequence analysis reported by Bazan (1990b). (B, bottom) Molscript (Kraulis, 1991) representation of the extracellular GRHR taken from the crystal structure of the GRHR−GRH complex (Brookhaven file pdb3HHR.ent). Loops not visible in the electron density map and not included in the model are indicated by dotted lines. After overlaying the IFNγR and GRHR amino acid sequences on this model according to the comparison of Bazan (1990b), the filled spheres show the residues in the GRHR that line up with the eight cysteine residues in the IFNγR. The eight cysteines in the IFNγR form four disulfide bonds: Cys^{60}−Cys^{68}, Cys^{105}−Cys^{150}, Cys^{178}−Cys^{183}, and Cys^{197}−Cys^{218} (Stüber et al., 1993).

and mouse IFNγR have been cloned and expressed (Aguet et al., 1988; Cofano et al., 1990; Gray et al., 1989; Hemmi et al., 1989; Kumar et al., 1989; Munro & Maniatis, 1989), and the full length soluble extracellular portion of the human IFNγR has been produced in *E. coli* and eukaryotic cells (Fountoulakis et al., 1990, 1991b; Gentz et al., 1992).

Four consecutive disulfide bonds are formed in the extracellular portion of the IFNγR between residues Cys^{60}−Cys^{68}, Cys^{105}−Cys^{150}, Cys^{178}−Cys^{183}, and Cys^{197}−Cys^{218} (Stüber et al., 1993). In a schematic model of the human IFNγ−IFNγR complex, based partly on the known GRH−GRHR crystal structure (De Vos et al., 1992), residues in both Ig-like domains, including a putative interdomain Cys^{105}−Cys^{150} disulfide (Figure 1B), were suggested to be directly involved in binding IFNγ (Stüber et al., 1993).

A large number of murine anti-IFNγR monoclonal antibodies have been described, including several that inhibit binding of IFNγ to the receptor (Aguet & Merlin, 1987; Garotta et al., 1990; Novick et al., 1987, 1989; Sheehan et al., 1988). These antibodies have been shown to recognize conformational epitopes, stabilized by one or more disulfides, in the vicinity of the IFNγ binding site (Garotta et al., 1990; Stüber et al., 1993). These high-affinity neutralizing monoclonal antibodies, either as fragments or in humanized forms, may be useful in the design of therapeutically active IFNγ antagonists for the potential treatment of autoimmune diseases, chronic inflammations, and allotransplant rejection (Ozmen et al., 1993).

We set out to determine whether the two putative Ig-like domains of the extracellular IFNγR can be produced separately as soluble proteins with a native-like fold, on the one hand to provide support for the predicted domain organization of this cytokine receptor, which is presently based largely upon a rather low sequence similarity to the extracellular GRHR (Bazan, 1990a,b), and on the other hand to localize the epitopes recognized by various neutralizing monoclonal antibodies. Of course, the availability of these domains also opens new avenues for structural studies that might benefit understanding of how IFNγ, the additional transmembrane receptor β-subunit, and the neutralizing monoclonal antibodies interact with the receptor α-chain.

MATERIALS AND METHODS

Chemicals and Enzymes. Cyanogen bromide activated Sepharose, protein-G Sepharose, and Q-Sepharose as well as Mono-Q and Superose-12 FPLC columns were purchased from Pharmacia. Bovine enterokinase was from Biozyme Laboratories (Great Britain) and had an activity of ≈150 units/μg. The synthesis of 11-mercaptoundecanoic acid was performed as described (Bain & Whitesides, 1990). Fradiomycin trisulfate (neomycin) was purchased from Fluka.

Plasmid Constructs. The following oligonucleotides were used for PCR (*Asp*718 and *Xba*I sites underlined):

Primer-1: 5′-GCAAGGTACCCGAGATGGGCAC-CGCGGATCTGGGG-3′

Primer-2: 5′-CATTCTAGATCATCCATCTCGGG-ATACAGCAAATTCTTCTGA-3′

Primer-3: 5′-GGCTTCTAGATCAAGAACCTTTT-ATACTGCTATTG-3′

Primer-4: 5′-GCAAGGTACCCGATGGAAAAAT-TGGACCACC-3′

Primer-5: 5′-GCAAGGTACCCGGACAAAAAGA-ATCTGCC-3′

Using primers-1 and -2 and the IFNγR cDNA as template (Aguet & Merlin, 1987), a DNA fragment encoding amino acids 1−108 in the mature receptor sequence was amplified by PCR, except that a mutation was introduced in the 3′-

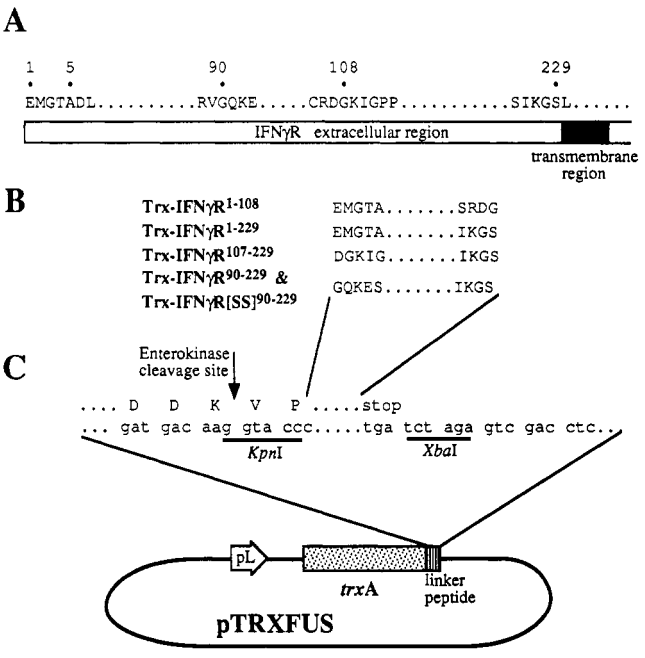

FIGURE 2: (A) Parts of the mature N-terminal IFNγR amino acid sequence from Glu^1 up to the first putative transmembrane residue (Leu^{230}). (B) Fragments of the IFNγR produced as thioredoxin fusion proteins. (C) pTRXFUS vector (LaVallie et al., 1993) and the cloning sites used to create the thioredoxin−IFNγR fusion proteins. Enterokinase cleavage of the fusion protein releases the receptor fragment with an additional two residues (Val-Pro) attached to the N-terminus.

primer to change the Cys^{105} to Ser^{105}. This oligonucleotide was cleaved by restriction endonucleases *Asp*718 and *Xba*I and cloned into the unique *Asp*718/*Xba*I sites in the plasmid vector pTRXFUS (LaVallie et al., 1993), to afford construct Trx−IFNγR^{1-108} (Figure 2). Using the same method and primer-1 and -3 afforded construct Trx−IFNγR^{1-229}, primer-4 and -3 gave Trx−IFNγ$R^{107-229}$, and primer-5 and −3 gave Trx−IFNγR^{90-229} (see Figure 2). Using primers-5 and -3 and, as a PCR template, plasmid DNA encoding a mutant receptor with residues 105 and 150 changed from Cys to Ser (Stüber et al., 1993), gave a thioredoxin-IFNγR fusion lacking the Cys^{105}−Cys^{150} disulfide (denoted below Trx−IFNγR[SS]$^{90-229}$). The PCRs were carried out under mineral oil in reaction buffer (100 μl) containing dNTPs (0.25 mM), $MgCl_2$ (1.5−3 mM), sense and anti-sense 5′-phosphate-kinased primers (100 pM), plasmid (0.01 pM), and AmpliTaq DNA polymerase (2 units). The reactions were performed using a Perkin Elmer 480 DNA thermal cycler as follows: 5 min at 95 °C, followed by 30 cycles of 1 min at 95 °C, 2 min at 55 °C, and 2 min at 72 °C. The PCR products were purified by agarose gel electrophoresis, rendered blunt-ended by treatment with T4 DNA polymerase I, and self-ligated to facilitate efficient restriction. The concatenated products were digested with *Xba*I and *Asp*718, and the resulting fragments were subcloned into the expression vector pTRXFUS. The genes assembled in this way were sequenced by the dideoxy method (Sanger et al., 1977) using a United States Biochemicals Sequenase sequencing kit according to the manufacturer's instructions. The plasmids were transformed into *E. coli* strains GI698 and GI724 for expression (Brent & Ptashne, 1981). All other recombinant DNA techniques followed standard protocols (Sambrook et al., 1989).

Production of Thioredoxin Fusion Proteins. E. coli GI724 containing the Trx−IFNγR construct of interest was grown at 30 °C in IMC broth with ampicillin (100 μg/mL) as described (LaVallie et al., 1993). Typically, cells were induced after they had grown to an OD of 0.5 at 550 nm by addition of tryptophan (100 μg/mL) and shaking was continued overnight (≈12 h). Cells were pelleted by centrifugation at 10000*g* for 15 min, resuspended in buffer (30 mL; 50 mM Tris, 2 mM EDTA, 1 mM PMSF, 1 mM benzamidine, pH 7.5), and sonicated on ice for 4 × 30 s. Cell debris was removed by centrifugation at 40000*g* for 1 h. After filtration (0.2 μm filter), Tris-HCl (50 mM) and NaCl (300 mM) were added, and the supernatant was loaded onto a column of Q-Sepharose (10 cm × 1.6 cm) and eluted with a gradient of NaCl (0.3−0.5 M over three column volumes). The fractions of interest were collected, concentrated by ultrafiltration, and dialyzed against Tris-HCl buffer (50 mM, pH 9).

An immunoaffinity column was prepared by linking either monoclonal antibody A1 or γR99 (10 mg) to cyanogen bromide activated Sepharose (1 mL), according to the manufacturer's protocol. Aliquots of protein containing the receptor fragment of interest were loaded, the column was washed with Tris-HCl (50 mM, pH 8), and the product was then eluted with glycine-HCl buffer (50 mM, pH 2.5), immediately neutralized by adding phosphate buffer (4 M, pH 7.2) and dialyzed against Tris-HCl (25 mM, pH 8).

The fusion protein was then chromatographed on a Mono-Q FPLC column equilibrated with Tris-HCl (25 mM, pH 8), eluting with a gradient of 0−0.5 M NaCl in the same buffer. The native-like Trx−IFNγR^{1-108} fusion protein was collected in a sharp protein peak at ≈0.25 M NaCl (Figure 3A), and the Trx−IFNγR^{90-229} and Trx−IFNγR[SS]$^{90-229}$ fusion proteins at ≈0.35 M NaCl.

Enterokinase Cleavage. The active fusion protein from the Mono-Q FPLC column was directly concentrated by ultrafiltration to an A_{280} of between 4 and 6. To a 1 mL aliquot was added 2000 units of bovine enterokinase. The course of the digestion at 28 °C could be followed by FPLC on a Mono-Q column (see above and Figure 3C). Typically, for the Trx−IFNγR^{1-108} fusion protein, the digestion proceeds cleanly to completion over 100−120 h. The 1 mL aliquot was then desalted into Tris-HCl buffer (25 mM, pH 8.0) by passage through a fast desalting column (Pharmacia) and chromatographed on a Mono-Q FPLC column using the conditions described above. The N-terminal receptor fragment elutes at ≈0.15 M and the thioredoxin at ≈0.2 M NaCl (Figure 3C). The IFNγR^{1-108} fragment shows an $A_{280} = 3.24$ at 1 mg/mL, according to quantitative amino acid analysis.

Refolding. Urea was added to the immunoinactive Trx−IFNγR^{1-108} fusion protein (peak B in Figure 3B) (2 mg/mL) in Tris buffer (50 mM, pH 8) to a final concentration of 7 M and DTT to 0.1 M. After 5 h at room temperature, the solution was dialyzed against Tris buffer (50 mM, pH 9) at 4 °C. Analysis of the product on a Mono-Q FPLC column (see above) showed a ≈1:1 ratio of active to inactive material. In the same way, the immunoinactive Trx−IFNγR^{90-229} fusion protein could be refolded to a ≈1:10 mixture of active and inactive material.

Gel Filtration. The IFNγR^{1-108} fragment was eluted through a Superose 12 gel filtration FPLC column equilibrated with sodium phosphate buffer (50 mM, pH 7.8), NaCl (150 mM), DTT (1 mM), and EDTA (1 mM) with a flow rate of 0.5 mL min^{-1}. The protein was loaded at a concentration of ≈500 μM. The column had been previously calibrated with *E. coli* thioredoxin (12 kDa), RNaseA (13.7

kDa), chymotrypsinogen (25 kDa), carbonic anhydrase (29 kDa), ovalbumin (43 kDa), and bovine serum albumin (67 kDa). The IFNγR$^{90-229}$ fragment was analyzed under similar conditions.

Antibodies. The murine monoclonal antibodies γR38, γR99, A1, A6, and D2 were raised against the native IFNγR (Aguet & Merlin, 1987; Garotta et al., 1990). They bind conformational epitopes on the receptor surface and inhibit the ligand binding capacity of the receptor. Antibodies γR38, A1, A6, and D2 recognize conformational epitopes within the N-terminal domain stabilized by the Cys^{60}–Cys^{68} disulfide, whereas the conformational epitope recognized by γR99 lies most likely between amino acids 53–193 and is stabilized in particular by the Cys^{178}–Cys^{183} disulfide (Stüber et al., 1993). The antibodies were produced in cell culture and purified by chromatography on protein-G Sepharose to >95% homogeneity, according to Coomassie blue stained 12% SDS–PAGE gels. The antibody concentration was determined by UV measurements using $A_{280} = 1.3$ as 1 mg/mL.

Biosensor Measurements. A home-built surface plasmon resonance apparatus was used (Huber et al., 1992, 1994). The sample flow through the microcell (0.5 μl) was 1 μL/s for antibodies A6, D2- and γR38 and 5 μL/s for antibody γR99. The flow was reduced to 0.3 μL/s to saturate the binding sites on the biosensor surface with high concentrations of antibody. The gold film on the sensor chip was modified as follows: The sensors were incubated overnight in a solution of 11-mercaptoundecanoic acid in methanol (2 mM). The resulting self-assembled monolayer is covalently linked to the gold surface via the sulfur atom (Bain & Whitesides, 1990). The exposed carboxylic acid groups were then activated with ethylchloroformate in dichloromethane (0.4 M) containing pyridine (0.5 M) and afterward derivatized with *N*-hydroxysuccinimide in pyridine (0.5 M). The chips were immersed in ethanol and subsequently in water and then incubated overnight in a solution of 20 mg/mL fradiomycin in sodium bicarbonate (0.2 M, pH 8.5). After being thoroughly rinsed in water, the chips were dried in a nitrogen stream. The free amino groups of the fradiomycin were reacted during 2 h with succinic anhydride (100 mM) and dimethylaminopyridine (1 mM) in dry pyridine. Again, the chips were rinsed with water and finally dried in a nitrogen stream. The immobilization of the IFNγR fragments was carried out on the biosensor apparatus in order to determine and control the amount of immobilized protein. The free carboxylic acid groups were activated in an aqueous solution of *N*-(3-dimethylaminopropyl)-*N*′-ethylcarbodiimide (100 mM) and *N*-hydroxysulfosuccinimide (25 mM) for 3–7 minutes. After washing with immobilization buffer (10 mM trisodium citrate, pH 5.1) and 2 M NaCl, the activated surface was contacted for 10 min with a 10–20 μg/mL solution of the receptor fragment to be immobilized, in immobilization buffer. The surface was washed with citrate buffer, the remaining *N*-hydroxysulfosuccinimide esters quenched with ethanolamine (1 M, pH 8.5), again washed with buffer, and finally the nonbound protein eluted out of the fradiomycin matrix by rinsing the surface with regeneration solution (10 mM HCl, 0.035% Triton X-100).

NMR and CD Measurements. ^{1}H NMR spectra were recorded on a Bruker AMX600 spectrometer at 300 K with 0.7 mM IFNγR$^{1-108}$ fragment in Tris-HCl (2 mM, pH 7.5) in 90% H_2O/10% D_2O with NaCl (15 mM). A total of 512 scans were accumulated with 4096 complex points and a spectral width of 8064 Hz. CD spectra were recorded on a Jasco J500-C instrument using a cuvette of 1 mm path length at 15 μM protein concentration in Tris-HCl (2 mM, pH 7.5) with NaCl (15 mM) at 288 K. Four to 16 scans were accumulated with a scan speed of 20 nm/min, a sample interval of 0.2 nm, and a time constant of 2 s. The spectra were smoothed by averaging 5–15 points.

Stability. Urea-induced denaturation of the IFNγR$^{1-108}$ fragment, which contains three tryptophan residues, was monitored by measuring the intrinsic fluorescence intensity of protein (1 μM) in Tris-HCl buffer (25 mM, pH 7.8) with NaCl (200 mM). Measurements were made in a 1.0 × 1.0 cm quartz cuvette thermostated at 24 °C in a Perkin Elmer LS50B spectrofluorimeter. Excitation was at 293 nm with slit widths 2.5 mm for excitation and 5 mm for emission. A urea stock solution (10 M) in Tris-NaCl buffer, prepared gravimetrically in a volumetric flask and adjusted to pH 7.8, was added to protein in buffer solution and incubated at 24 °C for 1.5 h prior to measurement. From each data set a background spectrum arising from buffer and urea components was subtracted.

RESULTS

Production of Thioredoxin-IFNγR Fusion Proteins. PCR-generated fragments of the human IFNγR cDNA were inserted into the *Asp*718 (isoschizomer of *Kpn*I) and *Xba*I cloning sites in the thioredoxin (Trx) gene fusion expression vector pTRXFUS, such that the coding nucleotide sequence for the receptor fragment was fused in-frame, through a linker, to the 3′-terminus of the *E. coli* thioredoxin gene (*trx*A) (LaVallie et al., 1993). The linker region encodes a peptide containing an enterokinase cleavage site (see Figure 2C).

Five different fragments were prepared by PCR (see Materials and Methods) and used to produce five fusion proteins (Figure 2B); clone-1 encodes residues 1–108 of the IFNγR and is designated Trx–IFNγR$^{1-108}$. This has the native IFNγR sequence except for mutation of Cys^{105} to Ser^{105}; clone-2 encodes the entire extracellular IFNγR from residues 1 to 229 (Trx–IFNγR$^{1-229}$); clone-3 encodes largely the putative membrane proximal domain of the receptor from residues 107–229 (Trx–IFNγR$^{107-229}$); clone-4 includes additional residues to the left and spans amino acids 90–229 (Trx–IFNγR$^{90-229}$) with the native sequence; and clone-5 spans the same 90 to 229 region but lacks the Cys^{105}–Cys^{150} disulfide (compare Figure 1B) due to site-specific double mutations at C105S and C150S (Trx–IFNγR[SS]$^{90-229}$).

The Trx–IFNγR$^{1-108}$ fusion protein was produced in substantial amounts (≈100 mg/L) in *E. coli* GI724 grown at 30 °C (but at greatly reduced levels in the same strain grown at 37 °C, or in *E. coli* GI698 at or below 30 °C). SDS–PAGE of sonicated cells indicated that most of the fusion protein was present in the soluble extract and not as insoluble inclusion bodies. The presence of some correctly folded IFNγR fragment in this extract was indicated by selective binding of a portion of the fusion protein to an A1-antibody-Sepharose immunoaffinity column. This immunoactive Trx–IFNγR$^{1-108}$ fusion protein eluted from a Mono-Q FPLC column largely in a single sharp peak (Figure 3A). When the crude soluble *E. coli* extract was assayed by chromatography on a Mono-Q column, the active and inactive portions of the fusion protein could be clearly seen in the

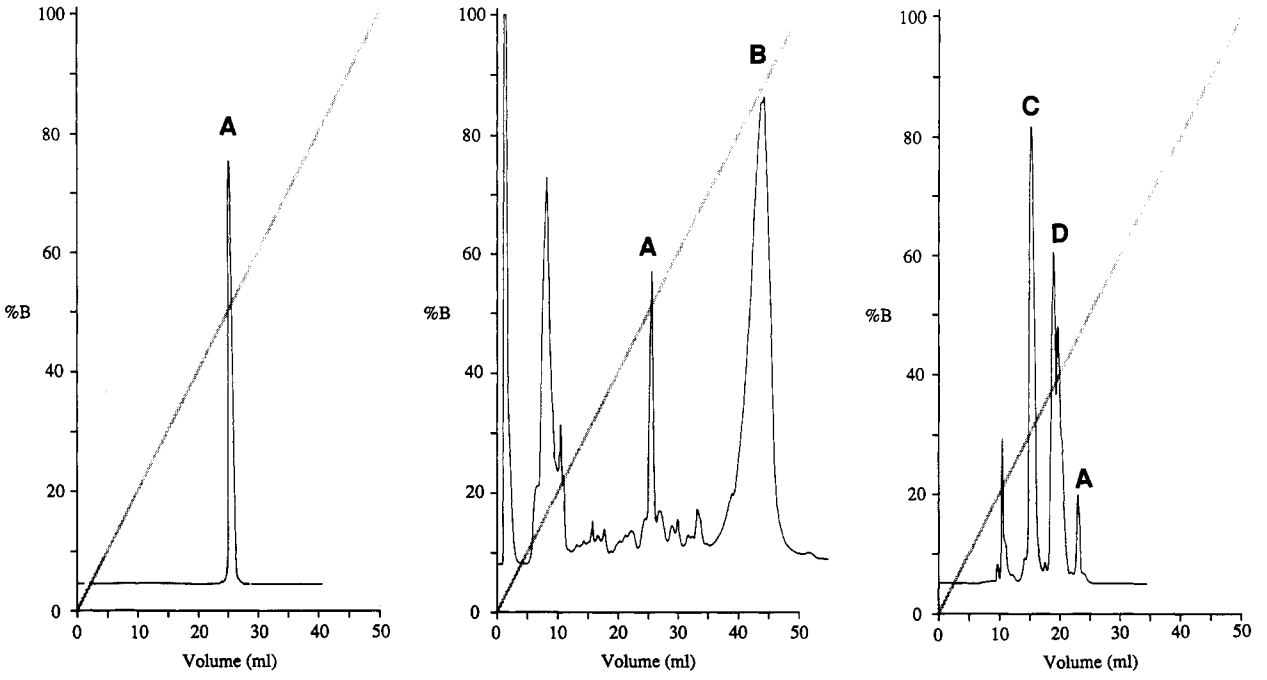

FIGURE 3: (A, left) FPLC chromatogram of the native-like Trx−IFNγR$^{1-108}$ fusion protein (peak A) eluted from a Mono-Q FPLC column (see Materials and Methods). (B, middle) FPLC chromatogram of a crude *E. coli* GI724(Trx−IFNγR$^{1-108}$) extract eluted from a Mono-Q column. Peak A is the native-like Trx−IFNγR$^{1-108}$ fusion protein, and peak B is the immunoinactive Trx−IFNγR$^{1-108}$ fusion protein (see text). (C, right) FPLC chromatogram of the Trx−IFNγR$^{1-108}$ fusion protein (peak A) after almost complete digestion with enterokinase; peak C = IFNγR$^{1-108}$; peaks D = fragments derived from Trx.

chromatogram, among the background of peaks from *E. coli* proteins (Figure 3B). The purified immunoactive and immunoinactive fusion proteins contained no free cysteines, based on quantitative Ellman tests (Ellman, 1959). When the cells were instead sonicated under reducing conditions, in the presence of 1 mM β-mercaptoethanol, the sharp peak corresponding to immunoactive material was absent from the chromatogram (peak A in Figure 3B), and none of the fusion protein present in the extract bound to the A1-immunoaffinity column. The presence of a 10:1 ratio of oxidized and reduced glutathione (5 mM GSSG, 0.5 mM GSH) during sonication had no effect on the amount of immunoactive fusion protein formed. The immunoactive Trx−IFNγR$^{1-108}$ fusion protein could be conveniently purified from soluble *E. coli* extracts (see Materials and Methods) in a yield of ≈15−20 mg/L and is stable over several weeks in phosphate buffered saline at 4 °C.

The immunoinactive Trx−IFNγR$^{1-108}$ fusion protein could be denatured in 7 M urea, reduced with DTT, and refolded by dialysis against Tris-buffer at 4 °C. This led to the recovery of active and inactive fusion protein in a ≈1:1 ratio. However, the purified receptor fragment IFNγR$^{1-108}$, produced by proteolytic cleavage of the fusion protein (vide infra), could not be refolded after denaturation and reduction under the same conditions. The presence of the thioredoxin fusion partner was needed to obtain efficient refolding of the reduced receptor domain.

The Trx−IFNγR$^{1-229}$ clone, containing eight cysteine residues in the receptor fragment, afforded very little fusion protein (<300 μg/L) that was bound directly from the cell extract by the A1-immunoaffinity column, although a large amount of immunoinactive material was detected in SDS−polyacrylamide gels of soluble *E. coli* extracts.

In an initial attempt to produce the membrane-proximal Ig-like domain, the Trx−IFNγR$^{107-229}$ fusion protein was expressed at 30 °C, under conditions that were optimal for the Trx−IFNγR$^{1-108}$ fusion protein. However, no protein could be isolated that bound to a γR99-Sepharose immunoaffinity column. Although residue 107 should lie in the interdomain linker region (Figure 1), residues to the left are thought to be necessary for binding γR99 (Garotta et al., 1990). Indeed, the Trx−IFNγR$^{90-229}$ construct in *E. coli* GI698 induced at 30 °C afforded soluble fusion protein which did bind to a γR99-Sepharose immunoaffinity column and could be eluted from a Mono-Q ion-exchange column as a single sharp peak (data not shown), although the yield was lower. A double C105S and C150S mutant (Trx−IFNγR-[SS]$^{90-229}$) was produced in the same way, which also bound to the γR99 immunoaffinity column. The immunoactive Trx−IFNγR$^{90-229}$ and Trx−IFNγR[SS]$^{90-229}$ fusion proteins, which did not contain free cysteines on the basis of the Ellman test (Ellman, 1959), were purified by the same procedure used for the Trx−IFNγR$^{1-108}$ construct, in yields of ≈1 mg/L of culture.

Enterokinase Cleavage of Fusion Proteins. The Trx−IFNγR$^{1-108}$ and Trx−IFNγR$^{90-229}$ fusion proteins were treated with enterokinase to release the receptor fragments together with two additional amino acids (Val-Pro) attached to their N-termini (Figure 2). The Trx−IFNγR$^{1-108}$ fusion protein was cleaved cleanly (Figure 3C), and the corresponding receptor fragment was easily recovered by chromatography on a Mono-Q FPLC column in high yield. The specific cleavage of the Trx−IFNγR$^{90-229}$ fusion protein proceeded less efficiently; more products were formed (data not shown) due to cleavage at other sites to the right within the 90−107 region, but the correct fragment could again be isolated by chromatography on a Mono-Q column. Automated N-terminal protein sequencing by the Edman method confirmed that both receptor fragments possessed the expected N-terminal amino acid sequences.

The IFNγR$^{1-108}$ fragment was eluted through a calibrated Superose 12 size exclusion column to estimate its molecular

weight. The protein was loaded as a 0.5 mM solution and eluted as a single sharp peak with an apparent mass of 13 kDa (calculated mass = 12.292 kDa), indicating that it exists largely as a monomeric protein up to almost millimolar concentrations. The IFNγR$^{90-229}$ fragment loaded as a $\approx$5 μM solution under the same conditions eluted with an apparent mass of 21 kDa, which is higher than its calculated mass (16.003 kDa). This may reflect a tendency for dimer formation, at this and higher concentrations, or the protein may be nonspherical due to the long N-terminal tail (residues 90−107) and thus migrate more rapidly.

Biosensor Measurements. A critical test of the correct folding of the receptor fragments is provided by comparing their dissociation constants (K_Ds) to the neutralizing antibodies γR38, A6, D2, and γR99, with those measured using native extracellular IFNγR produced in eukaryotic cells. SPR-biosensor technology is an ideal tool to determine accurately the K_Ds, in real time, with high sensitivity, without the need for labeled reagents (Liedberg et al., 1983; Löfås et al., 1991). In this method one partner of a given interacting "receptor−ligand" pair is immobilized on the sensor surface, and the other partner associates with and dissociates from the immobilized species and therefore changes the molecular surface coverage on the sensor continuously. This dynamic event can in the simplest case be described in terms of one pair of association and dissociation rate constants and an affinity constant, which are characteristic for the binding behavior of the two reaction partners.

The rate and the equilibrium constants were determined from biphasic experiments. A typical biphasic kinetic experiment—the binding of antibody A6 to IFNγR$^{1-108}$ fragment—is depicted in Figure 4A. First, the surface binding of the antibody at a defined, constant concentration in the range of the expected K_D was registered. The bulk antibody concentration was maintained constant by the very high sample flow (2−10 sample cell volumes per second). The maximal possible amount of antibody, ΔR_{max}, which could be bound by the respective immobilized receptor fragment was then determined using a high antibody concentration. After such an experiment the sensor surface was regenerated with HCl/Triton without losing activity for the following measurement.

The kinetic model from which the interaction constants were derived assumes reversible, monovalent complex (AB) formation between the immobilized receptor A and the dissolved ligand B:

$$A + B \rightleftharpoons AB \quad (1)$$

The binding reaction can therefore be formulated as a bimolecular association and a unimolecular dissociation reaction (Eddowes, 1987/88; Karlsson et al., 1991; Schlatter et al., 1993). The mathematical treatment of this process is described by

$$(d\Delta R/dt)_t = k_{on}\Delta R_{max}[C] - (k_{on}[C] + k_{off})\Delta R_t \quad (2)$$

where k_{on} and k_{off} are the association and dissociation rate constants, ΔR_{max} is the maximal surface coverage with ligand, ΔR_t is the surface coverage with ligand at time t, and [C] is the bulk concentration of ligand in solution. Provided that ΔR_{max} and [C] are known, the values for k_{on} and k_{off} can be calculated according to the linear relationship between ($d\Delta R/dt$) and ΔR_t from the intercept on the ordinate and from the slope of the straight line in the plot ($d\Delta R/dt$) versus ΔR_t (Figure 4B). The rate of binding ($d\Delta R/dt$) at any time corresponds to the slope of the binding curve and was calculated at the points indicated (Figure 4A) using an exponential function. The dissociation constant K_D and the affinity constant K_A can be calculated from the rate constants.

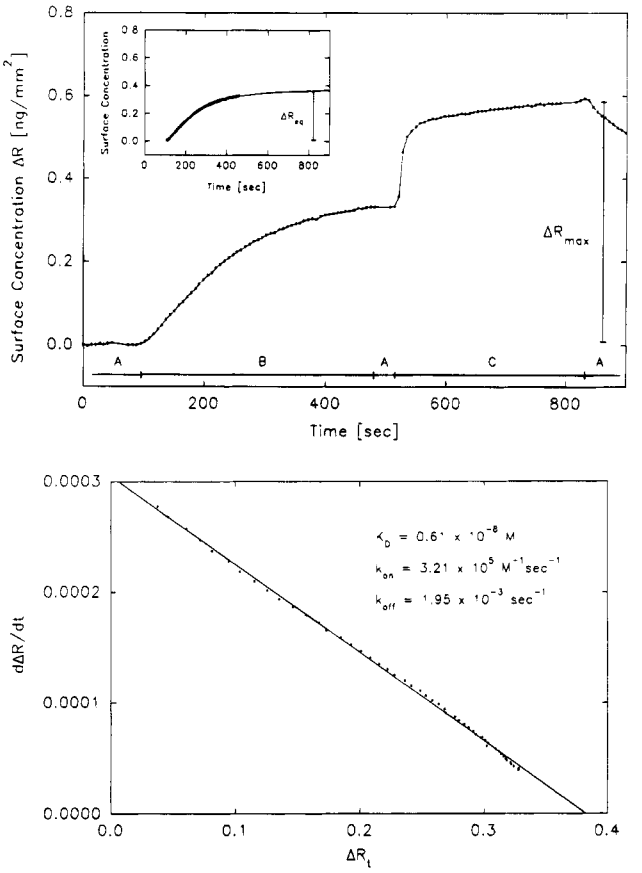

FIGURE 4: (A, top) Response curve showing the association of 1 × 10^{-8} M antibody A6 (B) and 2.5 × 10^{-6} M antibody A6 (C) with immobilized IFNγR$^{1-108}$. ΔR_{max} indicates the maximal amount of A6 bound by the immobilized receptor fragment (see text). The antibody dilutions were made in the running buffer, i.e., 50 mM sodium phosphate, pH 7.2, 150 mM NaCl, and 1% BSA (A). The binding curve is an interpolation between the experimental points, which were fitted to a monoexponential function. This function was used to calculate the binding rates at each of the measured points (bottom panel). Shown in the inset is the first part of the response curve, at 1 × 10^{-8} M antibody A6, and the fit of the curve to a monoexponential equation extrapolated to infinite time, corresponding to the equilibrium sensor response ΔR_{eq}. (B, bottom) Plot of the binding rate $d\Delta R/dt$ versus the amount of surface bound A6 (ΔR_t). The binding rate was calculated for each measured point, at 1 × 10^{-8} M A6, using an exponential function (panel A). The rate constants of the forward and the back reaction were obtained from the intercept on the ordinate and the slope of the linear regression through the calculated data points.

Perfect fitting of the response curve to a monoexponential equation indicates monovalent binding of the antibodies to the immobilized fragments. However, such monovalent binding takes place only if the intermolecular distance between the immobilized receptors is large enough to preclude bidentate binding through both antigen binding sites on the antibody, i.e., low amounts of protein must be immobilized. Low amounts of immobilized receptor protein are also advantageous to ensure that depletion of the sample solution at the surface does not occur. In these experiments, the observed maximal signals upon saturation of the sensor surface with antibodies A6, D2, and γR38 corresponded to

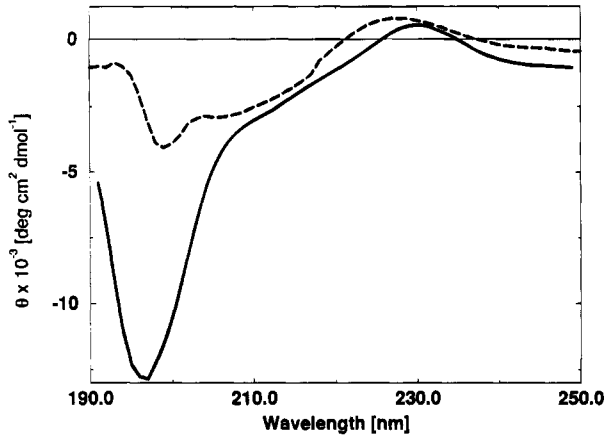

FIGURE 5: Circular dichroism spectra of the IFNγR$^{1-108}$ (solid line) and IFNγR$^{90-229}$ (broken line) receptor fragments (see Materials and Methods for measuring conditions).

approximately 10−20% of an antibody monolayer. In order to reliably determine the interaction constants for the γR99 antibody, even lower amounts of receptor fragment had to be immobilized. This was mainly necessary because of the very fast forward rate and the high affinity of γR99 for the receptor. The maximal saturation signal indicated that less than 5% of monolayer was formed. In addition, in order to avoid depletion of antibody from the very dilute sample solution, the sample flow using γR99 had to be at least 5 μL/s; a sample flow of 1 μL/s was used for antibodies A6, D2, and γR38. Only the low receptor density on the sensor surface combined with the high sample flow resulted in response curves which could be described with the standard monoexponential equation.

The interaction constants were determined from at least two experiments, and the calculated mean values are listed in Table 1.

CD Spectroscopy. The far-UV CD spectrum of the IFNγR$^{1-108}$ fragment between 190 and 250 nm shows a pronounced minimum at 194 nm, with a shoulder at 215 nm (Figure 5). Although the CD spectrum of IFNγR$^{1-108}$ deviates from that of an archetypal β-sheet, which normally shows a negative Cotton effect near 218 nm and a positive one around 195 nm (Yang et al., 1986), it is very similar in shape to the CD spectrum of recombinant extracellular GRHR (Bass et al., 1991) and the IFNγR from insect cells (Fountoulakis & Gentz, 1992). The CD spectrum of the IFNγR$^{90-229}$ fragment is similar (Figure 5).

NMR Spectroscopy. The 1D ^{1}H NMR spectrum of the IFNγR$^{1-108}$ fragment shows several features of a well-folded protein (Figure 6A). In particular, the high-field-shifted resonances between −0.3 and 0.6 ppm are typical for aliphatic methyl groups packed into the protein hydrophobic core. Ring currents in aromatic groups, among other effects, cause the upfield shift of aliphatic methyl resonances from the position near 1.0 ppm, where they are normally seen in random coil peptides or molten globules (Kuwajima, 1989). There are also numerous well dispersed low field amide proton resonances between 8.5 and 10 ppm and α proton resonances between 5 and 6 ppm that are indicative of β-sheet secondary structure (Wishart et al., 1992). In contrast, a sample of this IFNγR$^{1-108}$ fragment that after an extended period at 30 °C in low salt buffer was no longer recognized by the neutralizing antibodies, presumably due to unfolding, showed a ^{1}H NMR spectrum that was more typical of an unstructured protein (see Figure 6B). This

Table 1: Rate Constants (k_{on}, k_{off}) and Equilibrium Constants (K_D, K_A) Characterizing the Binding of Anti-IFNγR Antibodies to Immobilized IFNγR Fragments[a]

antibodies		IFNγR (eukaryotic)	Trx−IFNγR$^{1-108}$	IFNγR$^{1-108}$	Trx−IFNγR$^{90-229}$	Trx−IFNγR[SS]$^{90-229}$	IFNγR$^{90-229}$
A6	K_D (M)	(0.58 ± 0.13) × 10^{-8}	(0.25 ± 0.10) × 10^{-8}	(0.61 ± 0.21) × 10^{-8}	no binding	no binding	no binding
	K_A (M^{-1})	1.81 × 10^8	4.74 × 10^8	1.65 × 10^8			
	k_{off} (s^{-1})	2.19 × 10^{-3}	1.74 × 10^{-3}	1.95 × 10^{-3}			
	k_{on} (M^{-1} s^{-1})	3.96 × 10^5	7.21 × 10^5	3.21 × 10^5			
D2	K_D (M)	(0.77 ± 0.09) × 10^{-8}	(0.28 ± 0.04) × 10^{-8}	(0.67 ± 0.18) × 10^{-8}	no binding	no binding	no binding
	K_A (M^{-1})	1.32 × 10^8	3.52 × 10^8	1.49 × 10^8			
	k_{off} (s^{-1})	2.34 × 10^{-3}	0.94 × 10^{-3}	1.95 × 10^{-3}			
	k_{on} (M^{-1} s^{-1})	3.08 × 10^5	3.29 × 10^5	2.90 × 10^5			
γR38	K_D (M)	(4.09 ± 0.75) × 10^{-8}	(1.05 ± 0.03) × 10^{-8}	(3.15 ± 0.16) × 10^{-8}	no binding	no binding	no binding
	K_A (M^{-1})	0.25 × 10^8	0.96 × 10^8	0.32 × 10^8			
	k_{off} (s^{-1})	2.45 × 10^{-3}	1.01 × 10^{-3}	2.61 × 10^{-3}			
	k_{on} (M^{-1} s^{-1})	0.61 × 10^5	0.97 × 10^5	0.83 × 10^5			
γR99	K_D (M)	(0.06 ± 0.02) × 10^{-8}	no binding	no binding	(0.15 ± 0.03) × 10^{-8}	(0.18 ± 0.05) × 10^{-8}	(0.16 ± 0.06) × 10^{-8}
	K_A (M^{-1})	21.4 × 10^8			6.86 × 10^8	5.99 × 10^8	6.25 × 10^8
	k_{off} (s^{-1})	1.68 × 10^{-3}			6.65 × 10^{-3}	12.1 × 10^{-3}	4.89 × 10^{-3}
	k_{on} (M^{-1} s^{-1})	28.0 × 10^5			44.6 × 10^5	73.3 × 10^5	30.6 × 10^5

[a] The standard deviations for the K_D's are given. The mean values of all the data are determined from at least two experiments and vary less than about ±30%.

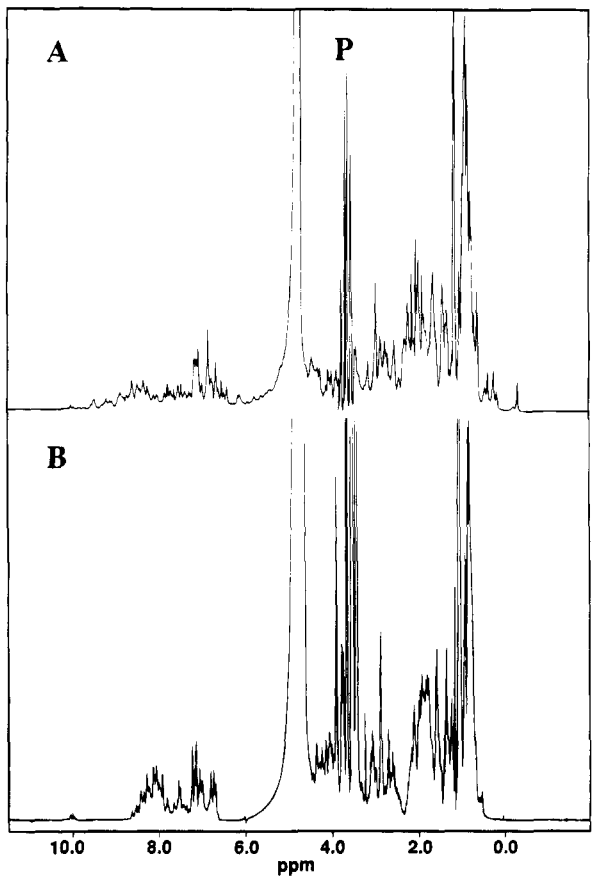

FIGURE 6: (A) ^{1}H NMR spectrum of the native-like IFNγR$^{1-108}$ receptor fragment. P indicates peaks arising from buffer components (see Materials and Methods for measuring conditions); (B) ^{1}H NMR spectrum of inactivated IFNγR$^{1-108}$ receptor fragment (see Results).

strengthens the correlation between binding activity to the antibodies and the need for a well folded native-like structure.

Stability. As mentioned above, the IFNγR$^{1-108}$ fragment could not be refolded after reduction with DTT and denaturation with urea, under conditions where the Trx–IFNγR$^{1-108}$ fusion protein can refold to the native state. However, as long as the disulfide bond is not reduced, the urea unfolded IFNγR$^{1-108}$ fragment quantitatively refolds to the native-like state upon removing the urea by dialysis. Fluorescence spectra of the native-like and denatured states in 6 M urea are shown in Figure 7A. The emission maximum is red-shifted from ≈346 to ≈355 nm and increases in intensity. Monitoring the decrease in emission at 316 nm with increasing urea concentration gives the denaturation curve shown in Figure 7B, indicating cooperative unfolding with a midpoint at 3.6 M urea. However, there is a larger and almost linear increase in fluoresence intensity with urea concentration at ≈360 nm. This emission spectrum must comprise overlapping bands from mainly the three Trp residues in the protein (Trp^{31}, Trp^{56}, and Trp^{82}). The observation of a cooperative unfolding transition strengthens further the conclusion that the IFNγR$^{1-108}$ fragment is a stable well-folded protein.

DISCUSSION

Within the sequence alignment of the extracellular IFNγR and GRHR reported by Bazan (1990b), amino acids that appear conserved for their structural role in predicted β-strands were grouped in blocks. Seven blocks were identified within the N-terminal ≈110 amino acids of each

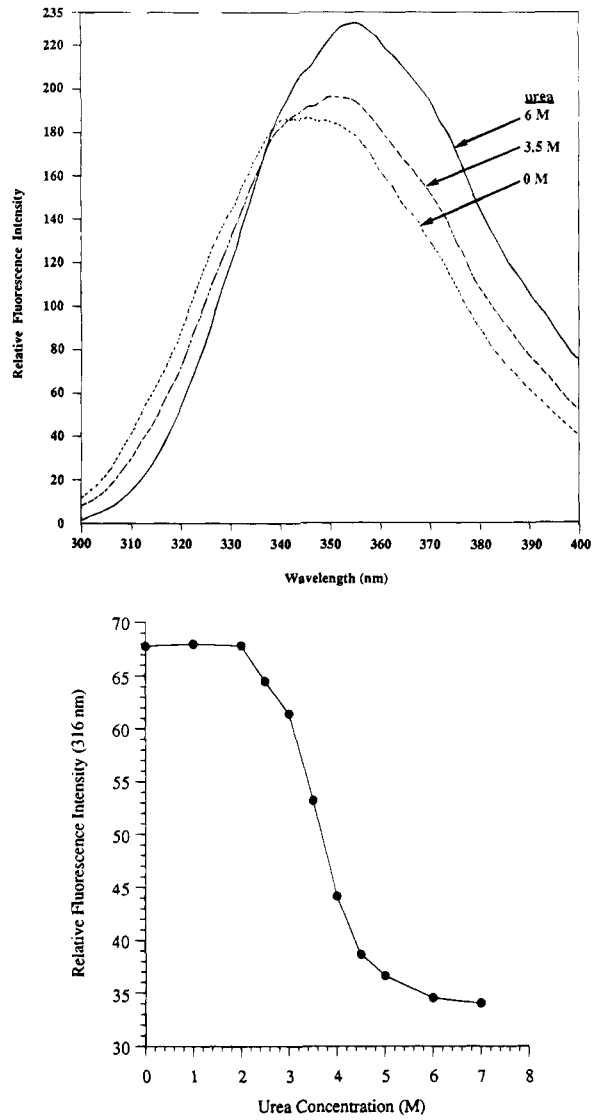

FIGURE 7: (A, top) Intrinsic fluorescence of the IFNγR$^{1-108}$ receptor fragment (excitation at 293 nm) in Tris-NaCl buffer at pH 7.8 and 0, 3.5, and 6 M urea. (B, bottom) Urea unfolding curve derived from changes in fluorescence emission at 316 nm. The curve is an interpolation between experimental points. The midpoint is at 3.6 M urea.

receptor, corresponding to seven β-strands, connected by intervening loop or turn sequences (Figure 1A). A second region extending over a further ≈110 residues was again divided into seven blocks representing seven putative β-strands in a second membrane proximal Ig-like domain. The crystal structure of the GRHR in a complex with GRH confirmed the two-domain structure for this receptor and revealed a short four-residue segment (Val^{125}Asp^{126}Glu^{127}-Ile^{128}) connecting the N- and C-terminal domains (De Vos et al., 1992). In the Bazan sequence comparison, these linker residues align with Val^{104}Cys^{105}Arg^{106}Asp^{107} in the IFNγR sequence.

The relevance of this comparison is strengthened by the following observation. Three of the four disulfide bonds in the extracellular IFNγR occur between cysteines that are not conserved at equivalent positions in the extracellular GRHR sequence. However, in the Bazan sequence comparison these three pairs of disulfide bonding cysteines in the IFNγR (Cys^{105}–Cys^{150}, Cys^{178}–Cys^{183}, and Cys^{197}–Cys^{218}) align with residues in the GRHR that, in the crystal structure of the GRHR receptor, are spatially adjacent and within or close

to disulfide bonding distance (Figure 1B). The remaining disulfide in the IFNγR ($Cys^{60}-Cys^{68}$) is conserved with one at the equivalent position in the GRHR ($Cys^{83}-Cys^{94}$) cross-linking strands C′ and E in the N-terminal domain.

On this basis, the complete N-terminal Ig-like domain of the IFNγR is predicted to extend approximately through amino acids 1−106, whereas the second membrane proximal Ig-like domain should extend from approximately residue 107 to 229.

The anti-IFNγR neutralizing antibodies γR38, γR99, A1, A6, and D2 used in this work recognize conformational epitopes on the receptor that are stabilized by one or more of the disulfide bonds. They do not bind the denatured and fully reduced receptor. The antibodies γR38, D2, A1, and A6 do not bind C60S or C68S receptor mutants (Stüber et al., 1993), indicating that an intact $Cys^{60}-Cys^{68}$ disulfide bond is needed for recognition by these antibodies. On the other hand, the antibody γR99 was shown earlier by immunoblotting to recognize an epitope lying between residues 53 and 193, whose conformation is stabilized in particular by the $Cys^{178}-Cys^{183}$ and partly also by the $Cys^{197}-Cys^{218}$ disulfide bonds (Stüber et al., 1993). However, mutation of Cys^{105} and Cys^{150} either singly or together to serine did not significantly affect binding to the antibodies used here. Thus the $Cys^{105}-Cys^{150}$ interdomain disulfide (Figure 1B) is not essential for their recognition. These conclusions are reinforced by earlier unfolding studies with partially and fully reduced forms of the IFNγR (Fountoulakis, 1992).

The experiments described in this paper show that the 108 amino acid N-terminal portion of the IFNγR ($IFN\gamma R^{1-108}$) can be produced in large amounts (≈100 mg/L) as a soluble thioredoxin fusion protein ($Trx-IFN\gamma R^{1-108}$) in the cytoplasm of *E. coli*. Although only 15−20% of this soluble fusion protein was produced directly in a native-like form, as shown by its recognition by the antibodies γR38, D2, A1, and A6, the remaining immunoinactive fusion protein could be reduced, denatured, and efficiently refolded to the immunoactive, native-like state. Since the active $IFN\gamma R^{1-108}$ receptor fragment, generated by enterokinase cleavage of the $Trx-IFN\gamma R^{1-108}$ fusion protein, did not refold to the native-like state under the same conditions, we conclude that the thioredoxin fusion partner most likely assists the reduced and denatured receptor domain to fold correctly. This would be consistent with the known ability of thioredoxin (Pigiet & Schuster, 1986) to behave like the homologous DsbA protein of *E. coli* and eukaryotic PDI, which can mediate fast disulfide interchange reactions and thereby facilitate protein folding (Nelson & Creighton, 1994; Weissman & Kim, 1993; Wunderlich et al., 1993). It has been shown recently that PDI promotes the correct folding of reduced antibody F_{ab} fragments (Lilie et al., 1994).

The single $Cys^{60}-Cys^{68}$ disulfide bond within the $IFN\gamma R^{1-108}$ receptor fragment appears to form spontaneously during the extraction procedure, since immunoactive $Trx-IFN\gamma R^{1-108}$ fusion protein is not found in cell extracts prepared under reducing conditions. The recovered immunoactive product, however, is stable under the same reducing conditions (1 mM β-mercaptoethanol). The fusion protein could be cleaved by enterokinase to release the $IFN\gamma R^{1-108}$ receptor fragment in high yield.

A second receptor fragment including residues 90−229 of the extracellular IFNγR, with three disulfide bonds, was made in a similar way. This region encompasses the second membrane proximal Ig-like domain, which is predicted to extend through residues 107−229 (Figure 1). However, the $Trx-IFN\gamma R^{90-229}$ fusion protein was produced less efficiently, and its cleavage by enterokinase also gave a lower yield of native-like $IFN\gamma R^{90-229}$ receptor fragment.

Surface plasmon resonance technology provides an ideal method to accurately monitor the relative affinities of the neutralizing antibodies for the isolated receptor domains and the intact extracellular IFNγR from eukaryotic cells. The relative affinities of the four antibodies—γR99, A6, D2, and γR38 from highest to lowest affinity—for the complete extracellular part of the IFNγR from eukaryotic cells are very similar to those for the receptor fragments and their fusion proteins (see Table 1). The binding pattern of the different antibodies is as predicted and confirms earlier investigations (Garotta et al., 1990). Antibodies A6, D2, and γR38 bind to the N-terminal receptor fragment $IFN\gamma R^{1-108}$, and γR99 does not, whereas the pattern is opposite for the membrane proximal domain $IFN\gamma R^{90-229}$, which binds γR99 but not A6, D2, and γR38. Moreover, A6, D2, and γR38 bind to the N-terminal receptor fragment $IFN\gamma R^{1-108}$ with affinities that are essentially identical to those seen with the intact receptor from eukaryotic sources, whereas γR99 binds to the $Trx-IFN\gamma R^{90-229}$ fusion protein and to the free $IFN\gamma R^{90-229}$ receptor fragment with only slightly lower affinities (by a factor of 2−3) than those seen to the full length native extracellular receptor. The kinetic data obtained for the $Trx-IFN\gamma R^{1-108}$ fusion protein indicate a somewhat higher affinity for A6, D2, and γR38, in comparison to the fragment alone or the complete extracellular receptor. The reasons for this are not known. The significantly higher affinity of γR99 for the receptor, compared to the other antibodies, is due largely to a faster on-rate. Finally, the $Trx-IFN\gamma R^{90-229}$ and the $Trx-IFN\gamma R[SS]^{90-229}$ fusion proteins bound to γR99 with comparable affinities, confirming that the $Cys^{105}-Cys^{150}$ disulfide is not essential for full recognition by γR99 (Stüber et al., 1993). The close agreement between the K_Ds found for γR99 are noteworthy given the technical difficulties encountered in accurately determining these high affinity interactions (see above).

That the two isolated receptor fragments, $IFN\gamma R^{1-108}$ and $IFN\gamma R^{90-229}$, are bound by these neutralizing antibodies with affinity constants which are very close to those observed with native full length extracellular receptor (Gentz et al., 1992) provides strong evidence for the presence in each domain of native-like structure. When each domain was tested for its ability to inhibit the binding of IFNγ to the native receptor on Raji cells, however, no significant inhibition could be detected up to a concentration of ≈15 μM (results not presented). This confirms earlier work (Fountoulakis et al., 1991a) which showed that a 25 kDa stretch of the extracellular portion of the receptor is required for full ligand binding capacity.

Further evidence that the $IFN\gamma R^{1-108}$ fragment is a stably folded protein with a native-like state comes from CD and NMR spectra, as well as urea induced unfolding studies (see Results). The far-UV CD spectrum (Figure 5) resembles closely in shape that of the intact extracellular human IFNγR expressed in insect cells (Fountoulakis & Genz, 1992), as well as the recombinant extracellular GRHR (Bass et al., 1991), all of which show a maximum negative Cotton effect between 195 and 200 nm. On the other hand, immunoglobulin light chain variable (V_L) and constant (C_L) fragments also show a negative cotton effect in CD spectra, but at a

higher wavelength, around 215−218 nm (Ikeda et al., 1968). This is consistent with a closer similarity in protein fold of the IFNγR to the GRHR than to antibody C_L and V_L domains. The lack of a distinct minimum at 222 nm indicates that the fragment contains little, if any, α-helical secondary structure. Also its 1D ^{1}H NMR spectrum shows features typical of a well-folded protein, rather than a random coil or molten globule (see Results and Figure 6). The CD spectrum of the membrane proximal IFNγR$^{90-229}$ fragment also resembles that of the IFNγR$^{1-108}$ fragment and the intact eukaryotic IFNγR, although its intensity is weaker. An insufficient amount of this IFNγR$^{90-229}$ fragment has been available so far for NMR studies. However, it may prove possible to optimize the production of a native-like membrane proximal IFNγR domain using this expression system by trimming amino acids from the N-terminus of the IFNγR$^{90-229}$ fragment and by replacing the interdomain disulfide-bonded cysteines (Cys^{105} and Cys^{150}) by serine (Figure 1).

Although we have not attempted to produce these IFNγR domains in other expression systems, the efficiency and ease of this thioredoxin gene fusion expression system for producing these Ig-like molecules in *E. coli* is noteworthy. Moreover, the yields of native-like protein may be improved by further optimization. The entire extracellular IFNγR has been produced previously in *E. coli*, but required extraction under denaturing conditions and subsequent refolding to obtain biologically active material (Fountoulakis et al., 1990). Moreover, this *E. coli* derived protein showed evidence of conformational heterogeneity, and its affinity for IFNγ was lower than that produced in eukaryotic cells (Gentz et al., 1992). Several other extracellular cytokine receptors have been produced in *E. coli*, including the entire extracellular GRHR, which was made in a soluble form by a secretion expression system (Fuh et al., 1990). However, in many cases the production of eukaryotic proteins in the cytoplasm of *E. coli* results in insoluble inclusion bodies (LaVallie et al., 1993).

These results show that the extracellular IFNγR can be dissected into two independent folding units, thus confirming the domain organization of the IFNγR predicted by Bazan (1990b). It is possible that the seven stranded β-sheet sandwich seen in each Ig-like domain of the GRHR crystal structure (Figure 1) is also conserved in the extracellular IFNγR, despite their rather low amino acid sequence similarity (20.8% identity). If this is the case, it will be interesting to understand how proteins at this relatively low level of similarity can adopt similar folds. At the least, significant conformational differences between these cytokine receptors may be expected in the loops connecting the β-strands, particularly if these are involved in ligand binding. The precise locations of amino acids in the receptor that directly contact IFNγ have not yet been defined (Axelrod et al., 1994). The availability of these IFNγR domains from a convenient *E. coli* expression system may facilitate structural (X-ray and NMR) and functional (mutagenesis) studies that address these and related questions.

ACKNOWLEDGMENT

We thank in particular Professor C. Weissmann for helpful discussions, Dr. D. Stüber for plasmids containing various parts of the IFNγR cDNA, Dr. M. Fountoulakis for help with biochemical assays, Dr. P. Hunziker (Biochemistry Institute, University of Zürich) for N-terminal protein sequencing, and Annelies Meier for expert technical assistance.

REFERENCES

Aguet, M., & Merlin, G. (1987) *J. Exp. Med. 165*, 988−999.
Aguet, M., Dembic, Z., & Merlin, G. (1988) *Cell 55*, 273−280.
Axelrod, A., Gibbs, V. C., & Goeddel, D. V. (1994) *J. Biol. Chem. 269*, 15533−15539.
Bain, C. D., & Whitesides, G. M. (1990) *Angew. Chem., Int. Ed. Engl. 28*, 506−512.
Bass, S. H., Mulkerrin, M. G., & Wells, J. A. (1991) *Proc. Natl. Acad. Sci. U.S.A. 88*, 4498−4502.
Bazan, J. F. (1990a) *Cell 61*, 753−754.
Bazan, J. F. (1990b) *Proc. Natl. Acad. Sci. U.S.A. 87*, 6934−6938.
Bohni, R., Hemmi, S., & Aguet, M. (1994) *J. Biol. Chem. 269*, 14541−14545.
Brent, R., & Ptashne, M. (1981) *Proc. Natl. Acad. Sci. U.S.A. 78*, 4204−4208.
Cofano, F., Moore, S. K., Tanaka, S., Yuhki, N., Landolfo, S., & Appella, E. (1990) *J. Biol. Chem. 265*, 4064−4071.
De Vos, A. M., Ultsch, M., & Kossiakoff, A. A. (1992) *Science 255*, 306−312.
Eddowes, M. J. (1987/88) *Biosensors 3*, 1−15.
Ellman, G. L. (1959) *Arch. Biochem. Biophys. 82*, 70−77.
Farrar, M. A., & Schreiber, R. D. (1993) *Annu. Rev. Immunol. 11*, 571−611.
Fountoulakis, M. (1992) *J. Biol. Chem. 267*, 7095−7100.
Fountoulakis, M., & Genz, R. (1992) *Biotechnology 10*, 1143−1147.
Fountoulakis, M., Juranville, J.-F., Stüber, D., Weibel, E. K., & Garotta, G. (1990) *J. Biol. Chem. 265*, 13268−13275.
Fountoulakis, M., Lahm, H.-W., Maris, A., Friedlein, A., Manneberg, M., Stueber, D., & Garotta, G. (1991a) *J. Biol. Chem. 266*, 14970−14977.
Fountoulakis, M., Schlaeger, E.-J., Gentz, R., Juranville, J.-F., Manneberg, M., Ozmen, L., & Garotta, G. (1991b) *Eur. J. Biochem. 198*, 441−450.
Fountoulakis, M., Zulauf, M., Lustig, A., & Garotta, G. (1992) *Eur. J. Biochem. 208*, 781−787.
Fuh, G., Mulkerrin, M. G., Bass, S., McFarland, N., Brochier, M., Bourell, J. H., Light, D. R., & Wells, J. A. (1990) *J. Biol. Chem. 265*, 3111−3115.
Garotta, G., Ozmen, L., Fountoulakis, M., Dembic, Z., Van Loon, A. P. G. M., & Stüber, D. (1990) *J. Biol. Chem. 265*, 6908−6915.
Gentz, R., Hayes, A., Grau, N., Fountoulakis, M., Lahm, H.-W., Ozmen, L., & Garotta, G. (1992) *Eur. J. Biochem. 210*, 545−554.
Gibbs, V. C., Williams, S. R., Gray, P. W., Schreiber, R. D., Pennica, D., Rice, G., & Goeddel, D. V. (1991) *Mol. Cell. Biol. 11*, 5860−5866.
Gray, P. W., Leong, S., Fennie, E. H., Farrar, M. A., Pingel, J. T., Fernandez-Luna, J., & Schreiber, R. D. (1989) *Proc. Natl. Acad. Sci. U.S.A. 86*, 8497−8501.
Greenlund, A. C., Schreiber, R. D., Goeddel, D. V., & Pennica, D. (1993) *J. Biol. Chem. 268*, 18103−18110.
Harlos, K., Martin, D. M. A., O'Brien, D. P., Jones, E. Y., Stuart, D. I., Polikarpov, I., Miller, A., Tuddenham, E. G. D., & Boys, C. W. G. (1994) *Nature 370*, 662−666.
Hemmi, S., Peghini, P., Metzler, M., Merlin, G., Dembic, Z., & Aguet, M. (1989) *Proc. Natl. Acad. Sci. U.S.A. 86*, 9901−9905.
Hemmi, S., Merlin, G., & Aguet, M. (1992) *Proc. Natl. Acad. Sci. U.S.A. 89*, 2737−2741.
Hemmi, S., Böhni, R., Stark, G., Di Marco, F., & Aguet, M. (1994) *Cell 76*, 803−810.
Hibino, Y., Kumar, C. S., Mariano, T. M., Lai, D., & Pestka, S. (1992) *J. Biol. Chem. 267*, 3741−3749.
Huber, W., Barner, R., Fattinger, C., Hübscher, J., Koller, H., Müller, F., & Schlatter, D. (1992) *Sensors Actuators B6*, 122−126.
Huber, W., Hurst, J., Schlatter, D., Steiner, B., Kouns, W. C., Barner, R., & Hübscher, J. (1994) *Eur. J. Biochem.* (in press).
Ikeda, K., Hamaguchi, K., & Migita, S. (1968) *J. Biochem. (Tokyo) 63*, 654−660.
Karlsson, R., Michaelsson, A., & Mattsson, L. (1991) *J. Immunol. Methods 145*, 125−133.

Kraulis, P. (1991) *J. Appl. Crystallogr. 24*, 946−950.
Kumar, C. S., Muthukumaran, G., Frost, L. J., Noe, M., Ahn, Y. H., Mariano, T. M., & Pestka, S. (1989) *J. Biol. Chem. 264*, 17939−17946.
Kuwajima, K. (1989) *Proteins: Struct., Funct., Genet. 6*, 87−103.
Langer, J. A., & Pestka, S. (1988) *Immunol. Today 9*, 393−400.
LaVallie, E. R., DiBlasio, E. A., Kovacic, S., Grant, K. L., Schendel, P. F., & McCoy, J. M. (1993) *BioTechnology 11*, 187−193.
Liedberg, B., Nylander, C., & Lundström, I. (1983) *Sensors Actuators 4*, 299−304.
Lilie, H., Mclaughlin, S., Freedman, R., & Buchner, J. (1994) *J. Biol. Chem. 269*, 14290−14296.
Löfås, S., Malmqvist, M., Rönnberg, I., Stenberg, E., Liedberg, B., & Lundström, I. (1991) *Sensors Actuators B5*, 79−84.
Muller, Y. A., Ultsch, M. H., Kelley, R. F., & de Vos, A. M. (1994) *Biochemistry 33*, 10864−10870.
Munro, S., & Maniatis, T. (1989) *Proc. Natl. Acad. Sci. U.S.A. 86*, 9248−9252.
Nelson, J. W., & Creighton, T. E. (1994) *Biochemistry 33*, 5974−5983.
Novick, D., Orchansky, P., Revel, M., & Rubinstein, M. (1987) *J. Biol. Chem. 262*, 8483−8487.
Novick, D., Fischer, D. G., Reiter, Z., Eshhar, Z., & Rubinstein, M. (1989) *J. Interferon Res. 9*, 315−328.
Ozmen, L., Gribaudo, G., Fountoulakis, M., Gentz, R., Landolfo, S., & Garotta, G. (1993) *J. Immunol. 150*, 2698−2705.
Pigiet, V. P., & Schuster, B. J. (1986) *Proc. Natl. Acad. Sci. U.S.A. 83*, 7643−7647.
Sambrook, J., Fritsch, E. F., & Maniatis, T. (1989) *Molecular Cloning: A Laboratory Manual*, Cold Spring Harbor Laboratory Press, Cold Spring Harbor, NY.
Sanger, F., Nicklen, S., & Coulson, A. (1977) *Proc. Natl. Acad. Sci. U.S.A. 74*, 5463−5467.
Schlatter, D., Barner, R., Fattinger, C., Huber, W., Hübscher, J., Hurst, J., Koller, H., Mangold, C., & Müller, F. (1993) *Biosensors Bioelectron. 8*, 109−116.
Sheehan, K. C. F., Calderon, J., & Schreiber, R. D. (1988) *J. Immunol. 140*, 4231−4237.
Soh, J., Donnelly, R. J., Kotenko, S., Mariano, T. M., Cook, J. R., Wang, N., Emanuel, S., Schwartz, B., Miki, T., & Pestka, S. (1994) *Cell 76*, 793−802.
Stüber, D., Friedlein, A., Fountoulakis, M., Lahm, H.-W., & Garotta, G. (1993) *Biochemistry 32*, 2423−2430.
Taga, T., & Kishimoto, T. (1992) *FASEB J. 6*, 3387−3396.
Weissman, J. S., & Kim, P. S. (1993) *Nature 365*, 185−188.
Wishart, D. S., Sykes, B. D., & Richards, F. M. (1992) *Biochemistry 31*, 1647−1651.
Wunderlich, M. W., Otto, A., Seckler, R., & Glockshuber, R. (1993) *Biochemistry 32*, 12251−12256.
Yang, J. T., Wu, C.-S. C., & Martinez, H. M. (1986) *Methods Enzymol. 130*, 208−269.

BI942064Q